Design and Performance Analysis of a Multi-level Fuzzy-Based Stabilizer to Dampen Low-Frequency Oscillation in Single-Machine Infinite Bus Systems

Tenaw Ayew Mezigebu(✉) and Belachew Bantyirga Gessesse(✉)

Faculty Electrical and Computer Engineering, Bahir Dar Institute of Technology, Bahir Dar University, Bahir Dar, Ethiopia
tenaway4488@gmail.com, belchwbbg1j1@gmail.com

Abstract. Power systems are frequently viewed as complex, nonlinear, and dynamic systems. This system is constantly subjected to small disturbances that can result in synchronization loss and system failure. To fix this issue, power system stabilizers are applied to generate extra excitation control signals. Conventional power system stabilizer (CPSS) is difficult to track the dynamic nature of the load since stabilizer gains are determined under specific working conditions. In this paper, a multi-level fuzzy-based stabilizer uses the variation of rotor speed and acceleration as an input to mitigate low-frequency oscillations (LFOs) in single-machine infinite bus systems. The system is represented mathematically by the Heffron Philips K-coefficients model. The controller's performance was investigated for disturbances exposed to inputs of various membership functions, such as a triangular, gaussian, generalized bell, and trapezoidal. Each membership function is compared. For instance, a multi-level fuzzy-based stabilizer with a triangular membership function settled the rotor angle, rotor speed, and electrical torque deviations 29.5%, 5.9%, and 39.7% faster than the gaussian membership function fuzzy-based PSS, respectively. The study's findings revealed that the triangular membership function performed better than other membership functions.

Keywords: LFOs · Multi-Level Fuzzy · Single-Machine System

1 Introduction

Power system stability is the capacity of a power system to establish restorative forces equal to or greater than the disturbing forces to preserve balance. This concept applies to the nation's interconnected power system since it is a highly nonlinear system that operates in a constantly changing environment where loads, generator outputs, and essential operating parameters change. Low-frequency oscillation is caused by an imbalance between the damping and synchronization torque in power systems, which modifies the generator voltage angle [1].

B. H. Woldegiorgis et al. (Eds.): ICAST 2022, LNICST 455, pp. 252–271, 2023.
https://doi.org/10.1007/978-3-031-28725-1_16

Small-signal stability, a subset of phase angle-related instability concerns, is the capacity of synchronous machines in an interconnected power system to maintain synchronism after being subjected to a slight disruption [2]. This occurs as a result of a balance between the electromagnetic and mechanical torques of each synchronous machine linked to a power system [3]. For instance, insufficient synchronizing torque results in "aperiodic" or non-oscillatory instability while inadequate dampening torque results in low-frequency oscillations [4]. Both of these small signal stability problems have resulted from poor damping caused by high gain voltage regulators to cancel the effect of synchronizing torque.

In excitation control, a high gain regulator has a binding effect of eliminating synchronizing torque but negatively affects the damping torque [5]. To solve the unwanted effect of these voltage regulators, other supplementary signals are introduced in the feedback loop. The additional signals are primarily caused by speed divergence, excitation divergence, or accelerating power, which is achieved by injecting a stabilizing signal into the excitation system, and the error signal drives the regulator [6].

The power system stabilizer is divided into three stages: lead-lag compensator, washout, and gain block [7]. To compensate for the lag between the PSS output and the subsequent electrical torque developed, lead-lag compensators use phase-lead circuits. A washout circuit functions as a high-pass filter. The amount of damping associated with rotor oscillation is determined by the gain of the power system stabilizer. Traditional control theory and a linearized system model are used to design conventional power system stabilizers (CPSS) that provide optimal behavior under fixed operating conditions [8]. A conventional controller, on the other hand, fails to achieve effective control in systems with frequently fluctuating parameters. These pique one's interest in developing a fuzzy logic controller (FLC). FLCs employ feasible reasoning, which is similar to how humans make decisions [9]. This enables knowledge and experience gained from the system to be applied in such a way that adequate control for the design is provided even when the system configuration and conditions change. As a result, control systems based on fuzzy logic can solve intelligent control tasks, adapt to changing environments, and make sound decisions [10]. A hybrid of the fractional PID controller and a single fuzzy logic-based stabilizer has been proposed to improve the stability of a single-machine infinite bus (SMIB) power system [11]. However, the controllers' capabilities are limited due to the need for an expert to design the best possible solution [12]. To address this issue, a type-2 fuzzy logic controller with more degrees of freedom to handle nonlinearities and uncertainties has been developed, improving power system stability [13]. The study's results, however, necessitated a complete mathematical model of the system, which was difficult due to the power system's dynamic and nonlinear nature. This triggers the researcher to find a new design to handle low-frequency oscillations with the best performance index when the systems are subjected to various small-signal disturbances.

2 Mathematical Modeling

Mathematical modeling of a power system consists of a synchronous machine, excitation, power system stabilizer, and multi-level fuzzy-based stabilizer.

2.1 Synchronous Machine Modeling

The complete model of the synchronous generator, which includes six electrical and two mechanical nonlinear dynamic equations, is shown below [14].

$$T'_{do}\frac{dE'_q}{dt} = -E'_q - (X_d - X'_d)\left[I_d - \frac{X'_d - X''_d}{(X'_d - X_{ls})^2}(\psi_{1d} + (X'_d - X_{ls})I_d + E'_q)\right] + E'_{fd} \tag{1}$$

$$T''_{do}\frac{d\psi_{1d}}{dt} = -\psi_{1d} + E'_q - (X'_d - X_{ls})I_d \tag{2}$$

$$T'_{qo}\frac{dE'_d}{dt} = -E'_d - (X_q - X'_q)\left[I_q - \frac{X'_q - X''_q}{(X'_q - X_{ls})^2}(\psi_{2q} + (X'_q - X_{ls})I_q + E'_d)\right] \tag{3}$$

$$T''_{qo}\frac{d\psi_{2q}}{dt} = -\psi_{2q} + E'_d - (X'_q - X_{ls})I_q \tag{4}$$

$$\frac{d\delta}{dt} = \omega - \omega_s \tag{5}$$

$$\frac{2H}{\omega_s}\frac{d\omega}{dt} = T_M - \frac{X''_d - X_{ls}}{(X'_d - X_{ls})}E'_qI_q - \frac{X'_d - X''_d}{(X'_d - X_{ls})}\psi_{1d}I_q - \frac{X''_q - X_{ls}}{(X'_q - X_{ls})}E'_dI_d + \frac{X'_q - X''_q}{(X'_q - X_{ls})}\psi_{2q}I_d - (X''_q - X''_d)I_dI_q - T_{FW} \tag{6}$$

where,

$E'_{d,q}$	Transient voltage in d-/q-axis	$T'_{do,qo}$	The transient time constant of d-/q-axis
E_{fd}	Field voltage	$T''_{do,qo}$	Sub transient time constant of d-/q-axis
H	Inertia constant	T_{FW}	Additional damping torque prop. to speed
$I_{d,q}$	Current in d-/q-axis	T_M	Mechanical torque
X_{ls}	Leakage reactance	$X'_{d,q}$	Transient reactance in d- /q-axis
δ	Rotor angle	$X''_{d,q}$	Sub transient reactance in d-/q-axis
ω	Rotor speed	ψ_{1d}	Flux linkage d-axis damper winding

Equations (1) and (2) describe the dynamics in the d-axis, while Eqs. (3) and (4) describe the dynamics in the q-axis. Equation (5) and (6) represents the well-known swing equations. The torque component T_{FW}, which introduces damping torque proportional to rotational speed, can be extra damping in all models.

2.2 Excitation System Model

The ST1A thyristor control model was used in the study because it allows negative field current to enable generator de-excitation, as shown in Fig. 1 [2].

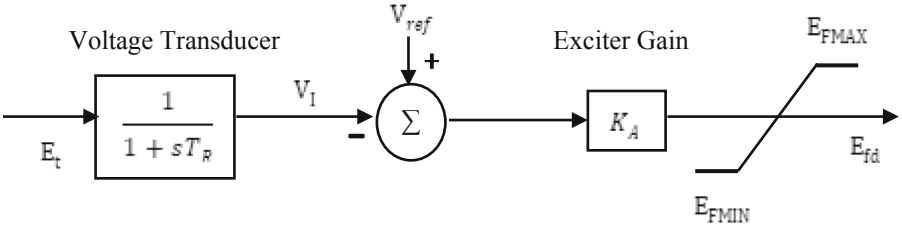

Fig. 1. Block diagram of an excitation system

A simplified model of ST1A excitation that is shown in Fig. 1, is linearized as:

$$\Delta E_t = \frac{e_{d0}}{E_{t0}}\Delta e_d + \frac{e_{q0}}{E_{t0}}\Delta e_q \tag{7}$$

$$E_{fd} = K_A(V_{ref} - V_I) \tag{8}$$

In terms of perturbed values;

$$\Delta E_t = K_A(-\Delta V_I) \tag{9}$$

In the preceding equations, Efd is the e.m.f. due to d-axis flux, and Vref is the steady-state magnitude of the terminal voltage. VR is the output voltage, and TR is the time constant.

2.3 Single-Line Diagram Representation of a Test System

In this study, the system that operates to the infinite bus is obtained in [6] and detailed machine constants are given in Appendix, as shown in Fig. 2, which is for simulation.

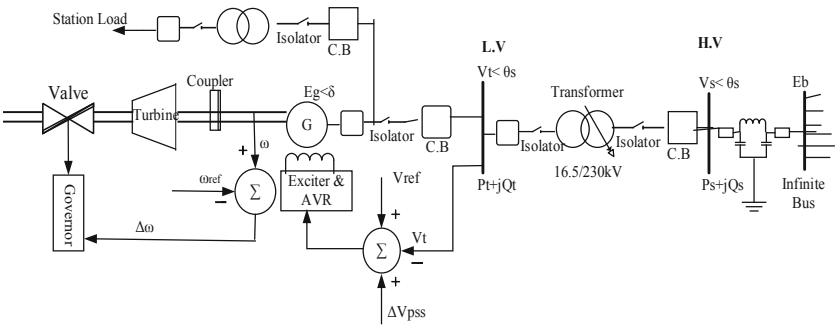

Fig. 2. A single-line diagram of the case study's single machine power system

The Heffron-Phillips model of the SMIB system shown in Fig. 3 is used in this paper [15]. H is the inertia constant, Δw is a deviation of speed, w_o is rated speed, s is the Laplace operator, K_1 to K_6 are known as K constants (which are the functions

of machine inertia constant, transmission line reactance, field time constant, machine loading conditions and exciter time constant), K_A is exciter gain, T_R, Tdo, and T_A are time constant of voltage transducer, field circuit, and exciter, respectively. The numerical values of the constants are given in Appendix.

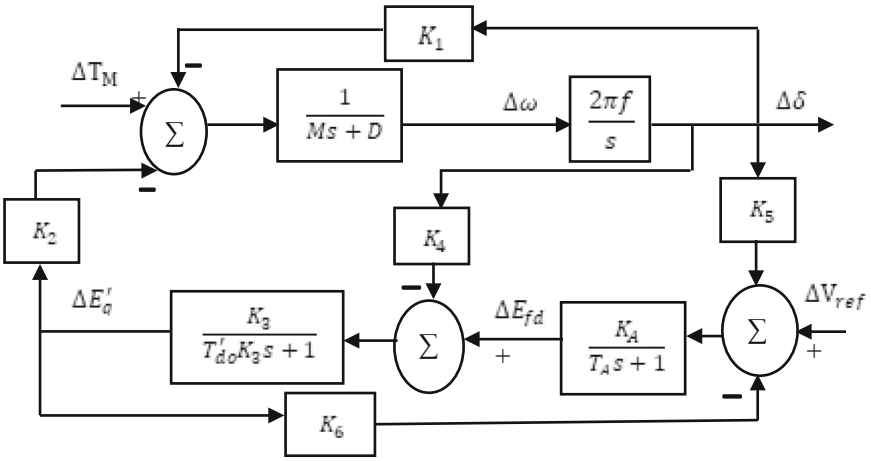

Fig. 3. A linearized model of a single machine connected to an infinite bus

2.4 Design of Conventional Power System Stabilizer

The expression of GEP(s) can be derived from Fig. 3 as follows [1]:

$$\mathrm{GEP(s)} = \frac{\mathrm{K_2K_3G_{exc}(s)}}{\left(1+\mathrm{sT'_{d0}K_3}\right)+\mathrm{K_3K_6G_{exc}(s)}} \tag{10}$$

The transfer function of the excitation system is as follows:

$$\mathrm{G_{exc}(s)} = \frac{K_A}{1+\mathrm{sT}_A} \tag{11}$$

Thus, Eq. (10) becomes:

$$\mathrm{GEP(s)} = \frac{\mathrm{K_2K_3K_A}}{\mathrm{T_AT'_{d0}K_3s^2}+\left(\mathrm{T_A}+\mathrm{T'_{d0}K_3}\right)\mathrm{s}+\mathrm{K_3K_6K_A}+1} \tag{12}$$

From Fig. 4, the contribution of the PSS to the torque-angle loop is given by:

$$\frac{\Delta \mathrm{T_{PSS}}}{\Delta\omega} = \mathrm{GEP(s)PSS(s)} \tag{13}$$

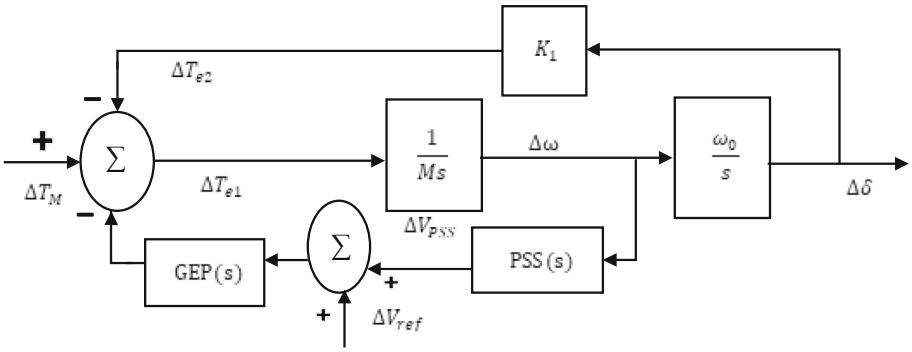

Fig. 4. Block diagram of a power system stabilizer with speed as an input

The state-space representation of the test system with exciter has become:

$$\begin{bmatrix} \Delta\dot{\delta} \\ \Delta\dot{\omega} \\ \Delta\dot{E}_q' \\ \Delta\dot{E}_{fd} \end{bmatrix} = \begin{bmatrix} 0 & \omega_s & 0 & 0 \\ -\frac{K_1}{2H} & -\frac{D\omega_s}{2H} & -\frac{K_2}{2H} & 0 \\ -\frac{K_4}{T_{do}'} & 0 & \frac{-1}{K_3 T_{do}'} & \frac{1}{T_{do}'} \\ -\frac{K_A K_5}{T_A} & 0 & -\frac{K_A K_6}{T_A} & -\frac{1}{T_A} \end{bmatrix} \begin{bmatrix} \Delta\delta \\ \Delta\omega \\ \Delta E_q' \\ \Delta E_{fd} \end{bmatrix} + \begin{bmatrix} 0 \\ 0 \\ 0 \\ \frac{K_A}{T_A} \end{bmatrix} \Delta V_{ref} \tag{14}$$

The eigenvalues of the system became calculated as:

$$|A - \lambda_i I| = 0;$$
$$\lambda_{1,2} = -0.0181 \pm 9.9433i;\ \lambda_{3,4} = -2.6971 \pm 10.8965i$$

where A denotes the system matrix, the corresponding damping factor (ξ) of the given SMIB is given in the Table 1 below.

Table 1. Damping ratio, undamped natural frequency, and frequency of oscillation

	Eigen values	σ	ω_n (rad/sec)	f (Hz)	ζ
$\lambda_{1,2}$	$-0.0181 \pm 9.9433i$	-0.0181	9.9433	1.582525	0.002
$\lambda_{3,4}$	$-2.6971 \pm 10.8965i$	-2.6971	10.8965	1.734232	0.2403

The eigenvalues obtained above prove that the system $\lambda_{1,2}$ is poorly damped compared with $\lambda_{3,4}$. So, a conventional power system stabilizer is applied to damp oscillation. During the conventional power system stabilizer design process, the following steps must be taken [15];

Step 1. Find the torque-angle loop's undamped natural frequency in rad/sec using the Heffron Philips model, ignoring all other sources of damping.

$$\frac{2H}{\omega_s} s^2 + K_1 = 0, \text{ i.e, } s_{1,2} = j\omega_n, \text{ where, } \omega_n = \sqrt{\frac{K_1 \omega_s}{2H}} = 10 \tag{15}$$

Step 2. Find the phase lag of GEP(s) at s = jωn in Eq. (10).

$$\mathrm{GEP(s)}\big|\mathrm{s}=_{\mathrm{j}\omega_{\mathrm{n}}} = \frac{49.374644}{11.597158 + 25.2342\mathrm{j}} = 1.78\angle -65.3174^{0} \tag{16}$$

Step 3. In Eq. (13) modify the phase lead of T(s) so that

$$\mathrm{T(s)}\big|\mathrm{s}=_{\mathrm{j}\omega_{\mathrm{n}}} + \mathrm{GEP(s)}|@\mathrm{s} = j\omega_n = 0 \tag{17}$$

Let

$$\mathrm{T(s)} = \mathrm{K_{PSS}}\left(\frac{1+\mathrm{sT_1}}{1+\mathrm{sT_2}}\right)^{\mathrm{k}} \tag{18}$$

Ignoring the washout filter time constants (T1 and T2), whose net phase contribution is approximately zero, k = 1 when T1 > T2. Now select T1, and T2 as some values between 0.02 and 0.15 s [1]. As a result, for T2 = 0.0575 s, their corresponding T1 values are:

$$\begin{aligned} &\angle(1+\mathrm{j10T_1}) = \angle\left[(1+\mathrm{j10}*0.0575) - 1.78\angle -65.3174^{0}\right] \\ &10T_1 = \tan\left(83.3213^{0}\right); \\ &\mathrm{T_1} = \frac{\tan\left(83.3213^{0}\right)}{10} = 0.854\,\mathrm{s} \end{aligned} \tag{19}$$

Step 4. The phase lead of G(s) cancels the phase lag caused by GEP(s) at the oscillation frequency, and the contribution of the PSS via GEP(s) is a pure damping torque with a damping coefficient DPSS.

$$\mathrm{D_{PSS}} = 2\xi\omega_{\mathrm{n}}\mathrm{M} = \mathrm{K_{PSS}}\big|\mathrm{T(s)}\big|\mathrm{s}=_{\mathrm{j}\omega_{\mathrm{n}}}\big|\mathrm{GEP(s)}|@\mathrm{s} = j\omega_n \tag{20}$$

From Eq. (18), find KPSS, knowing $\boldsymbol{\omega}_n$ and the desired [1].

$$\mathrm{K_{PSS}} = \frac{2\xi\omega_{\mathrm{n}}\mathrm{M}}{\big|\mathrm{T(s)}\big|\mathrm{s}=_{\mathrm{j}\omega_{\mathrm{n}}}\big|\mathrm{GEP(s)}\big|\mathrm{s}=_{\mathrm{j}\omega_{\mathrm{n}}}} = \frac{2*0.25*10*2*2.37}{6.65*0.9978*1.78} = 2$$

As a result, the final conventional power system stabilizer would be:

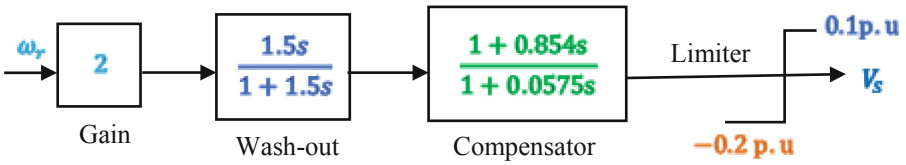

Fig. 5. Block diagram of a designed conventional power system stabilizer

The conventional power system stabilizer, as shown in the above figure (Fig. 5), is made up of three blocks: phase compensation, signal washout, and gain. The phase compensation block provides the appropriate phase-lead characteristics to compensate for the phase lag between exciter input and generator electrical torque. The signal washout block acts as a high pass filter, removing DC signals. PSS damping is determined by the stabilizer gain.

2.5 Design of Multi-level Fuzzy Logic Controller-Based Stabilizer

Low-frequency oscillations in a power system are damped using additional control signals sent to an automatic voltage regulator (AVR) via a speed deviation signal [16]. The rotor speed and its derivative are used as inputs, and the output is a voltage signal [17]. The fuzzy logic controller output has been multiplied by Kout again to give the appropriate control signal ΔV [18]. Blocks of the fuzzy logic controller with normalization factors are given in Fig. 6. The scaling factors Kin1 and Kin2 are the normalization factors for rotor speed and rate of the speed, respectively.

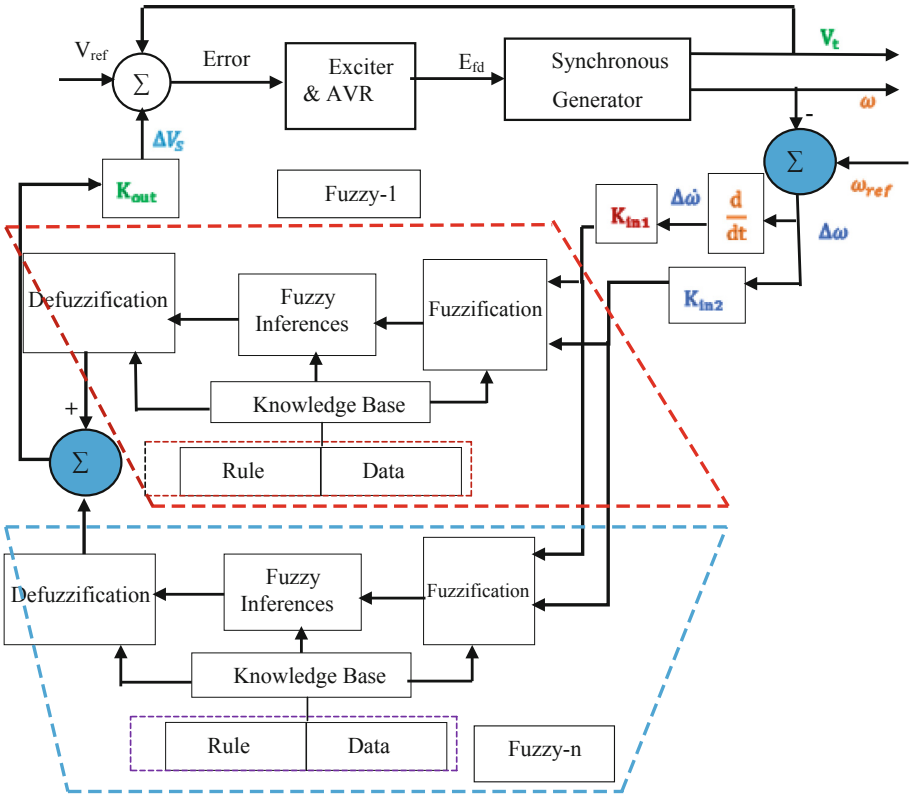

Fig. 6. Block diagram of proposed multi-level fuzzy-based stabilizer

The input domain can be described by linguistic terms such as positive big (PB), positive medium (PM), positive small (PS), zero (Z), negative small (NS), negative medium (NM), and negative big (NB) for seven linguistic variables [19].

Fuzzy Rule Base. A rule that describes the relationship between the input and output of fuzzy controllers can be set up using accessible knowledge in designing PSS [20]. The rule base is built using prior knowledge from plant dynamics, existing controllers, and experienced experts [18].

Rule 1. If the speed deviation is NB and the acceleration is PB, the voltage (output of fuzzy PSS) is NS. This means when the load angle and rotor acceleration decrease, the excitation system reduces the field voltage required to stabilize the system.

Rule 2. If speed deviation is NM and acceleration is NB, then a voltage (output of fuzzy PSS) is NB.

Rule 3. If speed deviation is PS and acceleration is PS, then a voltage (output of fuzzy PSS) is PS, and so on. This means when the load angle and rotor acceleration increase, the excitation system raises the field voltage needed to stabilize the system.

Table 2 explains all 49 rules that govern the mechanism wherever all symbols are defined in basic fuzzy logic expressions.

Table 2. Fuzzy logic control rule bases [19]

Acceleration / Speed	Voltage						
	NB	NM	NS	Z	PS	PM	PB
NB	NB	NB	NB	NB	NM	NM	NS
NM	NB	NM	NM	NM	NS	NS	Z
NS	NM	NM	NS	NS	Z	Z	PS
Z	NM	NS	NS	Z	PS	PS	PM
PS	NS	Z	Z	PS	PS	PM	PM
PM	Z	PS	PS	PM	PM	PM	PB
PB	PS	PM	PM	PB	PB	PB	PB

3 Simulation Results

The performance of the SMIB system with only the excitation system, conventional PSS (lead-lag), single fuzzy, and multi-level-fuzzy based PSS is analyzed using the Heffron Philips (K constant) values. A step input signal is used as the prime mover for a synchronous generator in the Simulink model.

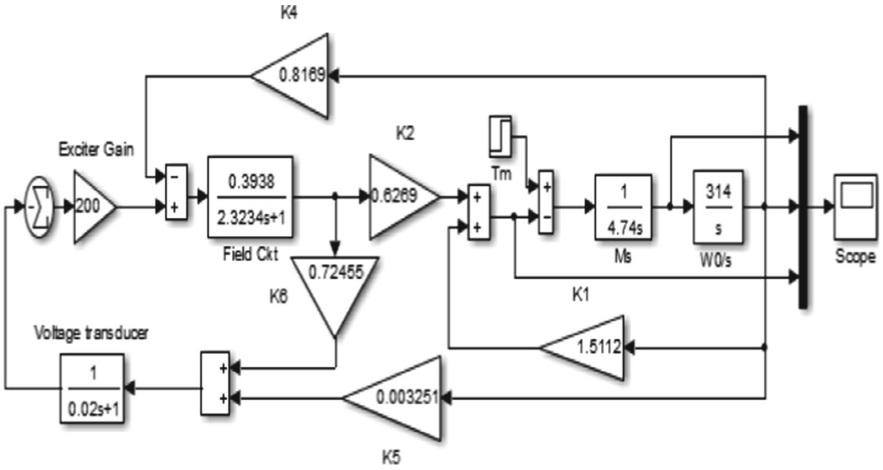

Fig. 7. SIMULINK model with AVR

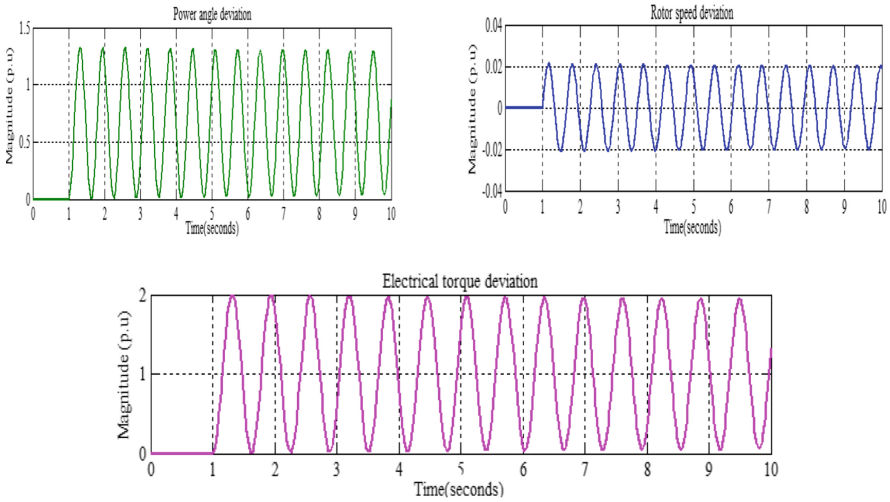

Fig. 8. Response of a 100% step-change in T_M without PSS

3.1 System Performance with Excitation System Only

Figure 7 shows the Simulink block with only the excitation system for the test system.

The response of the system without any controller applied is as follows:

As illustrated in Fig. 8, the system's response has oscillatory due to an insufficient damping coefficient. Without any stabilizer, the settling time of power angle, rotor speed, and electrical torque deviations takes more than 100 s. As time goes up, the oscillating amplitude decreases but persists for an extended time, causing the system to become monotonically unstable. This results in the equipment to be loss of synchronism or

being damaged so to protect the system from this proper power system stabilizer became designed.

3.2 System Performance with Conventional Power System Stabilizer

Figure 9 below shows the Simulink block diagram of the conventional power system stabilizer for the system. The numerical values of the power system stabilizer block are determined in the design section.

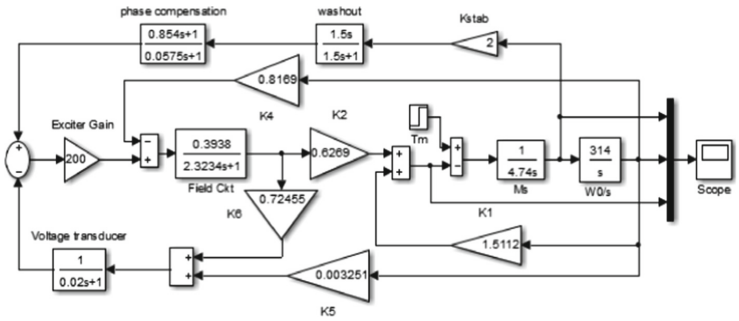

Fig. 9. SIMULINK model with power system stabilizer

Figure 10 shows the response of the system with conventional stabilizers when there is a 100% step change in mechanical torque.

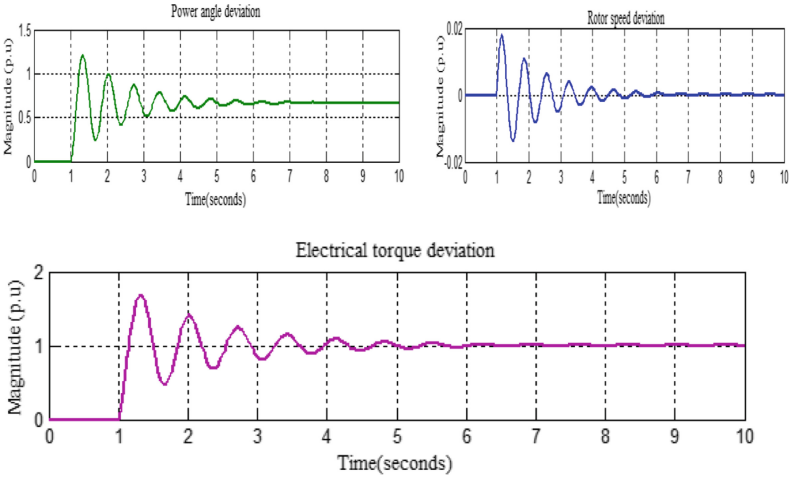

Fig. 10. Response of a 100% step-change in T_M with CPSS

As shown in Fig. 10, the settling time for rotor angle, rotor speed, and electrical torque deviations is 6.3019, 6.4544, and 5.9409 s, respectively. This showed that the designed

stabilizer able to settle small signal disturbances within 7 s. As a result, conventional power system stabilizers reduced the settling time by 93.698%, 93.546%, and 94.059% for rotor angle, rotor speed, and electrical torque deviations, respectively, improving the low-frequency oscillations as compared with the existing system without any stabilizer.

3.3 System Performance with Fuzzy Logic-Based Stabilizer

The Simulink model of a single fuzzy logic controller to damp small signal oscillations in a single-machine infinite bus system can be shown in Fig. 11.

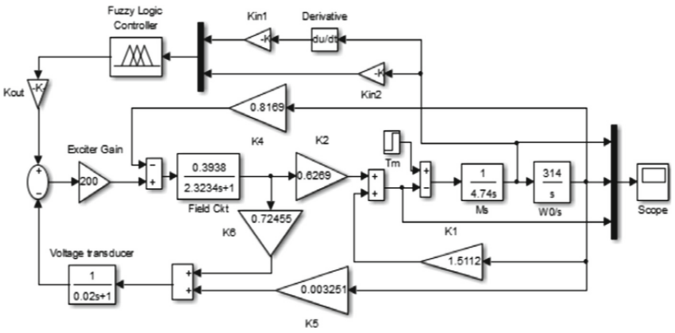

Fig. 11. SIMULINK model with a single fuzzy logic-based stabilizer

When there is a 100% step change in mechanical torque in the system, the response of rotor angle, rotor speed, and electrical torque deviation with a single fuzzy-based power stabilizer is shown in Table 3 with different membership functions below.

Table 3. The response of the system via a single fuzzy logic-based stabilizer

Controller	Membership function	
	Triangular	Gaussian
Single fuzzy	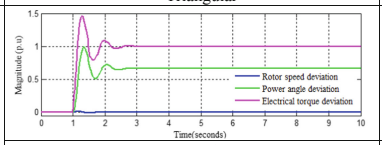	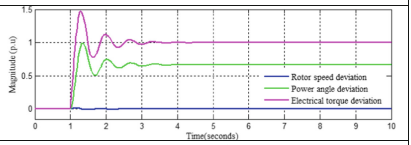
	Generalized Bell	Trapezoidal
	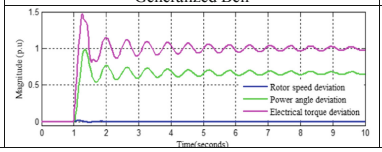	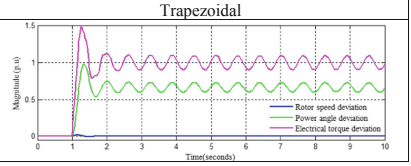

From Table 3, the settling time of electrical torque deviations for a single fuzzy-based power system stabilizer with triangular and gaussian membership functions is 2.4478

and 3.0769 s, respectively, to reach a steady-state value. This indicated that the fuzzy controller enhances small signal disturbance with minimum time and overshoot as compared to the conventional stabilizer that was seen in the previous session. This makes a single fuzzy with triangular and gaussian membership function-based power system stabilizer achieved settling time by 58.797% and 48.208% earlier than conventional power system stabilizers, respectively, for electrical torque deviations. This stated that triangular membership settles 10.589% quicker than gaussian membership. The response of the system for power angle deviations via a single fuzzy with triangular and gaussian membership function-based stabilizer achieved a settling time of 59.757% and 50.578% faster than conventional stabilizers, respectively. Therefore, the triangular membership function achieved the settling time 9.179% quicker than the gaussian membership function. While a single fuzzy with generalized bell and trapezoidal membership function-based power system stabilizer achieved a settling time of 67.670% and 158.325% slower than conventional power system stabilizers, respectively. This perceived that generalized bell and trapezoidal membership resulted in oscillatory amplitude decreases but persist for a long time even slower than conventional stabilizer. Due to this generalized bell and trapezoidal membership single fuzzy-based stabilizer is not advisable to improve LFOs.

3.4 System Performance with Multi-level Fuzzy Logic-Based Stabilizer

The SIMULINK model builds to study the performance of a multi-level fuzzy logic controller to damp LFOs is given in Fig. 12. The proposed controller incorporates the intelligent metaheuristic optimization algorithm to optimize the parameters of the system in addition to the direct fuzzy controller.

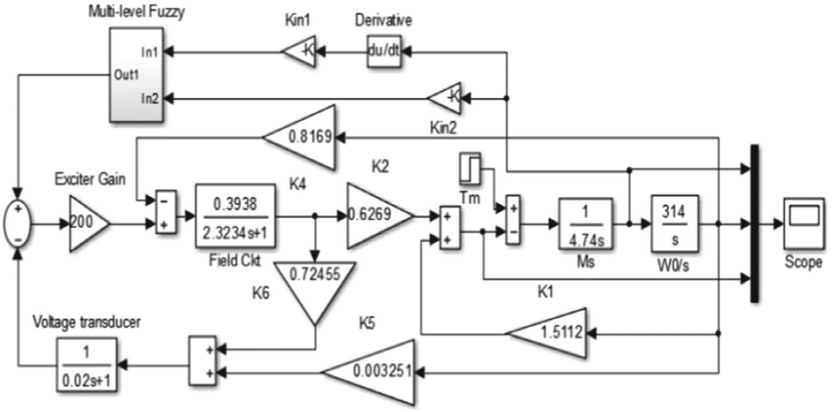

Fig. 12. SIMULINK model with multi-level fuzzy logic-based PSS

Table 4 illustrates the response of the multi-level fuzzy-based power system stabilizer to dampen low-frequency oscillations for various membership functions.

Table 4. The response of the test system via a multi-level fuzzy logic-based stabilizer

Controller	Membership function	
	Triangular	Gaussian
Single fuzzy	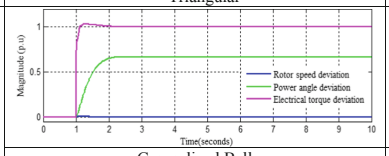	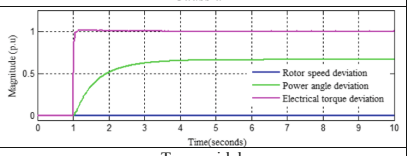
	Generalized Bell	Trapezoidal
	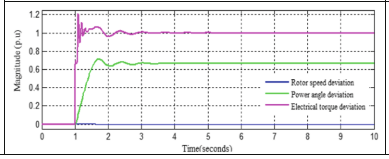	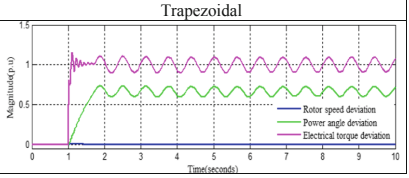

As per results from Table 4, the settling time of electrical torque deviations using a multi-level fuzzy-based stabilizer with triangular, gaussian, and generalized bell membership functions takes 0.0627, 0.6376, and 1.4155 s, respectively, to reach the final steady-state value. This showed that the designed stabilizer can settle small signal disturbances in the smallest time as compared to any stabilizer mechanism. As a result, a multi-level fuzzy with triangular, gaussian, and generalized bell membership function-based power system stabilizer settled 95.670%, 55.961%, and 2.231% faster than a single fuzzy with triangular fuzzy-based power system stabilizer. The response of the system for power angle deviations via a multi-level fuzzy-based stabilizer with triangular and gaussian membership settled 34.601% and 5.084% quicker than a single fuzzy-based stabilizer. While the settling time of electrical torque deviations for a multi-level fuzzy-based power system stabilizer with a trapezoidal membership function takes more than 100 s. Consequently, the oscillatory output is produced by a multi-level fuzzy with trapezoidal membership function-based power system stabilizer. Due to this, trapezoidal membership multi-level fuzzy-based stabilizer is not applicable to improve LFOs. Thus, Multi-level fuzzy improves power system stability and removes steady-state error that occurs in the system within a short time. This, in turn, increases the reliability, quality, and security of the power system.

3.5 Comparative Analysis of the System

The comparative analysis response graph of electrical torque and power angle deviation among various stabilizers via various membership functions with a 5%, 25%, 50%, 75%, and 100% change in mechanical torques is given in Table 5.

Table 5. Comparison of system response with performance index via various stabilizers

Membership	Parameter response for 5% change in mechanical torque	
	Electrical torque deviation	Load angle deviation
Triangular	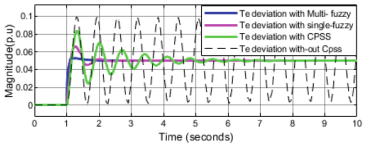	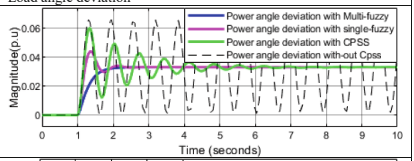
Gaussian	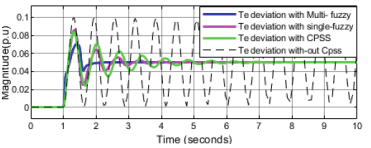	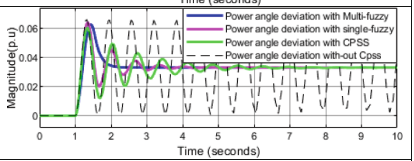
Generalized Bell	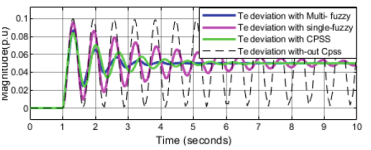	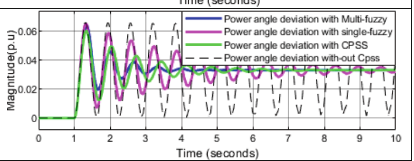
Trapezoidal	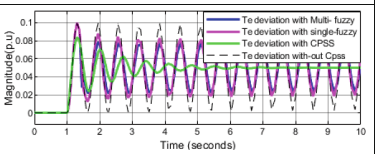	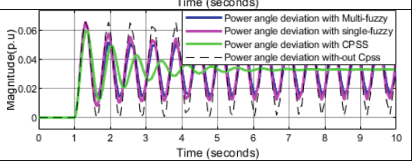
Membership	Parameter response for 25% change in mechanical torque	
	Electrical torque deviation	Load angle deviation
Triangular	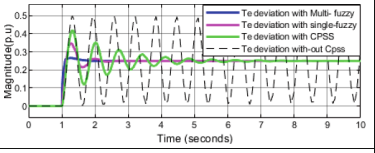	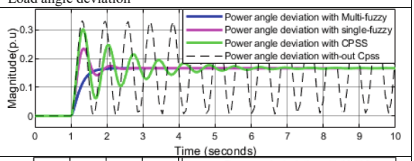
Gaussian	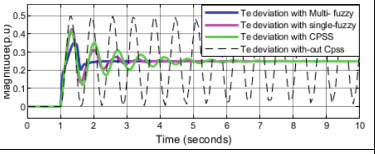	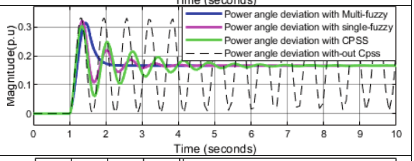
Generalized Bell	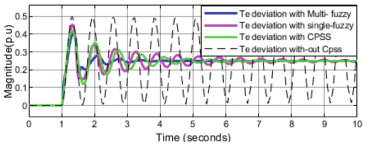	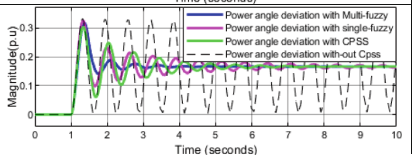

(*continued*)

Table 5. (*continued*)

Trapezoidal	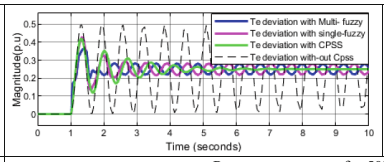	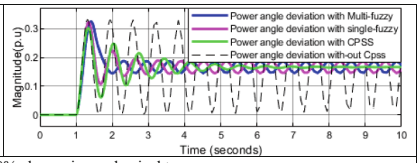
Membership	Parameter response for 50% change in mechanical torque	
	Electrical torque deviation	Load angle deviation
Triangular	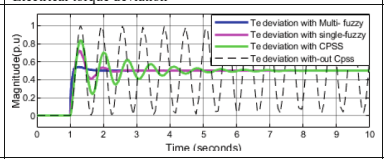	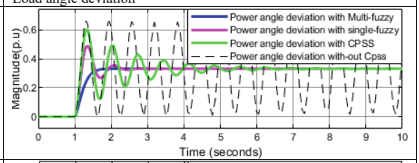
Gaussian	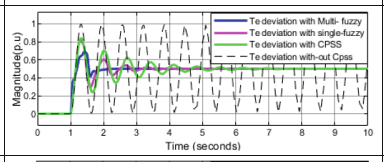	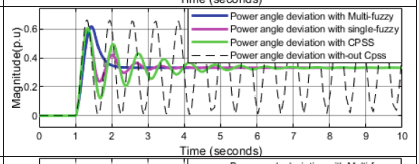
Generalized Bell	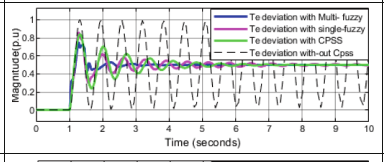	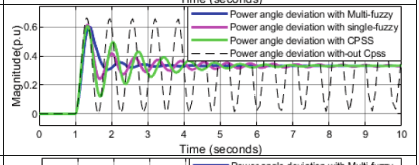
Trapezoidal	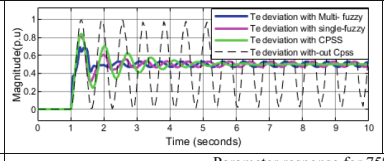	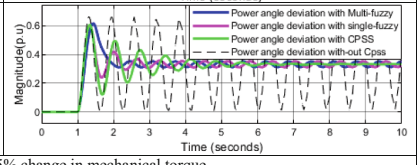
Membership	Parameter response for 75% change in mechanical torque	
	Electrical torque deviation	Load angle deviation
Triangular	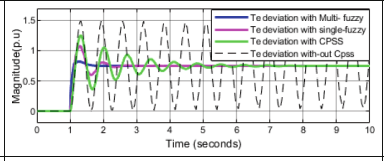	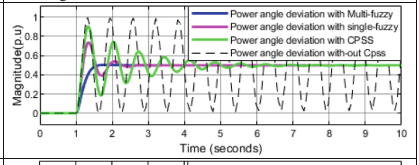
Gaussian	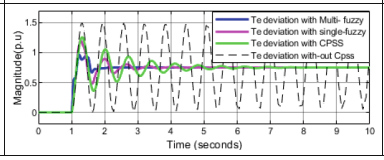	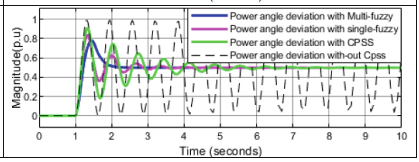

(*continued*)

Table 5. (*continued*)

Membership	Parameter response for 100% change in mechanical torque	
	Electrical torque deviation	Load angle deviation
Generalized Bell	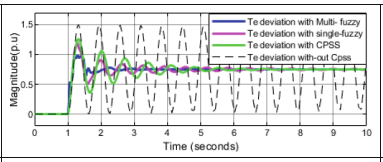	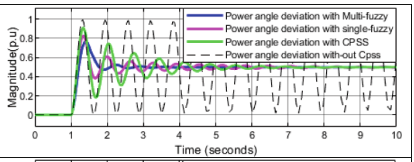
Trapezoidal	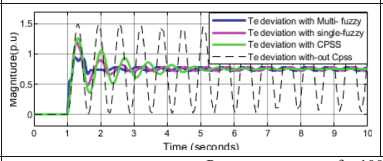	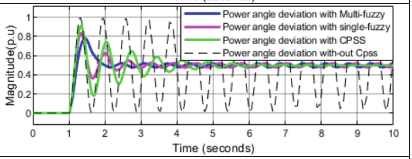
Triangular	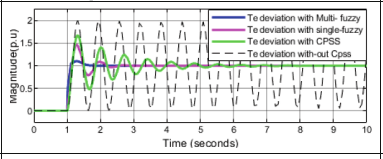	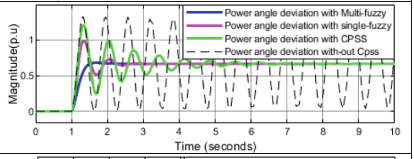
Gaussian	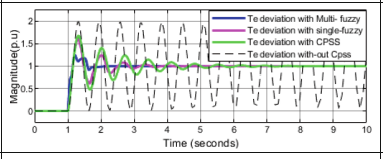	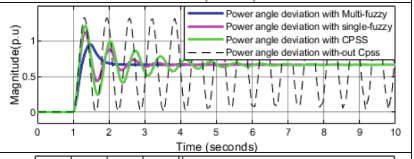
Generalized Bell	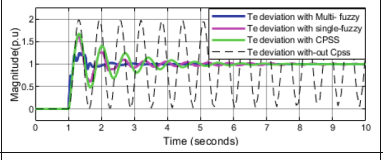	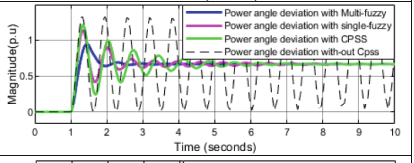
Trapezoidal	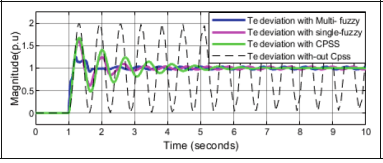	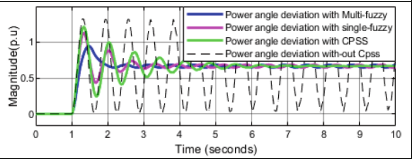

From the above response curve, it can be perceived that with the application of a fuzzy logic-based stabilizer improves the overshoot and settling time of the system as compared to AVR and CPSS. The application of a multi-level fuzzy stabilizer to the system not only improves small signal stability with small overshoot, but it is also robust to track the dynamic nature of the loads with zero steady-state error in a short time. This, in turn, increases the reliability, quality, and security of a system. The performance index via different stabilizers can be summarized in tabular form.

Table 6. Comparison of system response with performance index via various stabilizers

	ΔT_e			$\Delta\delta$			$\Delta\omega$		
Controller	Maximum peak(Mp)	Overshoot(%)	Settling time(sec.)	Maximum peak(Mp)	Overshoot(%)	Settling time(sec.)	Maximum peak(Mp)	Overshoot(%)	Settling time(sec.)
AVR	1.9899	98.9879	>100	1.3222	99.0020	**> 100**	0.0211	2.111	**> 100**
CPSS	1.6724	67.2440	5.9409	1.2131	82.5834	6.3019	0.01794	1.794	6.4544
Single-Fuzzy (Triangular)	1.4590	45.8972	2.4478	0.9899	48.9853	2.5361	0.0147	1.470	2.6456
Single-Fuzzy (Gaussian)	1.4722	47.2172	3.0769	0.9960	49.9022	3.1145	0.0148	1.480	3.2802
Single-Fuzzy (Gen-Bell)	1.4815	48.1502	9.9611	0.9805	47.5702	9.9630	0.0149	1.490	13.5371
Single-Fuzzy (Trapezed-)	1.4997	49.9669	**> 100**	0.9890	48.8586	**> 100**	0.0149	1.490	**> 100**
Multi-Fuzzy (Triangular)	**1.0167**	**1.6722**	**1.0627**	**0.6645**	**0.0182**	**2.0046**	**0.0027**	**0.270**	**2.2008**
Multi Fuzzy (Gaussian)	1.0295	2.9630	1.6376	0.6658	0.2146	2.4580	0.00404	0.404	2.2960
Multi Fuzzy (Generalized Bell)	1.2101	21.0061	2.4155	0.7122	7.1947	3.8457	0.0055	0.550	3.8599
Multi Fuzzy (Trapezoidal)	1.1976	19.7631	**> 100**	0.7345	10.5442	**> 100**	0.0048	0.480	**> 100**

According to Table 6, the settling time of electrical torque deviations, a multi-level fuzzy with triangular, gaussian, and generalized bell membership function-based stabilizer was 95.670%, 55.961%, and 2.231% quicker than a single fuzzy with triangular fuzzy-based stabilizer. This shows a triangular membership-based multi-level fuzzy stabilizer settled 39.709% quicker than a gaussian.

The settling time of power angle deviations by Multi-level Fuzzy with triangular and gaussian membership functions achieved 34.601% and 5.084% quicker than a single fuzzy with a triangular-based stabilizer, respectively for a 25% change in mechanical torque. As a result, a triangular membership-based stabilizer settled 29.517% faster than a gaussian. While the settling time of power angle deviations via multi-level fuzzy with generalized bell and trapezoidal membership function was achieved by 85.255% and 641% slower, respectively, than a single fuzzy with triangular-based stabilizer.

The multi-level fuzzy with triangular and gaussian membership function-based achieved settling time by 27.030% and 21.245%, respectively, quicker than a single fuzzy with triangular single fuzzy-based stabilizer for rotor speed deviation. As a result, a triangular-based stabilizer settled 5.785% faster than a gaussian. Therefore, a multi-level fuzzy-based stabilizer with triangular membership effectively enhances LFOs with the smallest overshot, peak amplitude, and settling time as compared with others.

4 Conclusion

This paper is developed to dampen low-frequency oscillations in a single-machine system via a multi-level fuzzy logic controller-based stabilizer. The study was simulated using a MATLAB/SIMULINK model and the performance was compared with a single fuzzy and conventional stabilizer. The system response via a conventional power system

stabilizer achieved a settling time of 93.698%, 93.546%, and 94.059% quicker than with AVR for rotor angle, rotor speed, and electrical torque deviations, respectively. While the performance of a single fuzzy with triangular and gaussian membership function-based stabilizer achieved the settling time 58.797% and 48.208% earlier than conventional power system stabilizer, respectively. Contrary to this, the performance of multi-level fuzzy with triangular, gaussian, and generalized bell membership function-based stabilizers achieved the settling time 95.670%, 55.961%, and 2.231% quicker than a single fuzzy, respectively. Therefore, the application of multi-level fuzzy to the system with a triangular membership settled 29.517%, 5.785%, and 39.709% quicker than gaussian for rotor angle, rotor speed, and electrical torque deviations, respectively. The proposed multi-level fuzzy controller is robust and most effective to damp LFOs with small settling time, overshot and steady error and the result of the study has relevant to improve the power quality, reliability, and security of the power system.

5 Appendices

Appendix A: Parameters of Single Machine Infinite Bus Power System (in p.u) [2]

$H = 2.37\ s$	$D = 0$	$KA = 200$	$Rs = 0$
$\omega s = 314\ rad/s$	$Xe = 0.7\ pu$	$TA = 0.2\ s$	$Xq = 1.64\ pu$
$T'_{d0} = 5.90\ s$	$Re = 0.02\ pu$	$Xd = 1.70\ pu$	$X'_d = 0.245\ p.u$
$V_\infty = 1.00 \angle 0\ pu$	$V_t = 1.72 \angle 19.31\ pu$		

Appendix B: Computation of Heffron-Philips's constant (K_1-K_6)

$$A = (X_e + X_q)(X'_d + X_e) + {R_e}^2 = 2.2117$$

$$K_1 = -\frac{1}{A}[V_\infty\{(X'_d - X_q)I_d - E_q\}\{(X_e + X'_d)\cos\delta + R_e\sin\delta\} + V_\infty(X'_d - X_q)I_q\{(X_e + X_d)\sin\delta - R_e\cos\delta\}] = 1.5112$$

$$K_2 = \frac{1}{A}[E'_q R_e + I_q A - I_q(X'_d - X_q)(X_e + X_q) - R_e(X'_d - X_q)I_d = 0.6269$$

$$K_3 = \frac{1}{\left(1 + \frac{(X_d - X'_d)(X_e + X_q)}{A}\right)} = 0.3938$$

$$K_4 = \frac{V_\infty(X_d - X'_d)}{A}[(X_e + X_q)\sin\delta - R_e\cos\delta] = 0.8169$$

$$K_5 = \frac{1}{A}\left\{\frac{V_{d0}X_q}{V_{t0}}\{V_\infty(X_e + X'_d)\cos\delta_{s0} + V_\infty R_e\sin\delta_{s0}\} + \frac{V_{q0}}{V_{t0}}[V_\infty X'_d\{R_e\cos\delta_{s0} - (X_e + X_q)\sin\delta_{s0}\}]\right\} = 0.003251$$

$$K_6 = \frac{1}{A}\left\{\frac{V_{d0}}{V_{t0}}R_e X_q - \frac{V_{q0}}{V_{t0}}X'_d(X_e + X_q)\right\} + \frac{V_{q0}}{V_{t0}} = 0.72455$$

References

1. Anderson, P.M., Fouad, A.A.: Power System Control and Stability, 3rd edn. Wiley, Ames, Iowa (2019)

2. Mondal, D., Chakrabarti, A., Sengupta, A.: Power System Small Signal Stability Analysis and Control, 2nd edn. Academic Press, London (2020)
3. Zhu, Y.: Power system loads and power system stability. Springer, Cham (2020). https://doi.org/10.1007/978-3-030-37786-1
4. Kumar, Y., Mishra, R.N., Anwar, A.: Enhancement of small signal stability of SMIB system using PSS and TCSC. In: 2020 International Conference on Power Electronics & IoT Applications in Renewable Energy and its Control (PARC), pp. 102–106. IEEE (2020)
5. Li, G., Zhang, J., Wu, X., Yu, X.: Small-signal stability and dynamic behaviors of a hydropower plant with an upstream surge tank using different PID parameters. IEEE Access **9**, 104837–104845 (2021)
6. Kundur, P.S., Balu, N.J., Lauby, M.G.: Power system dynamics and stability. Power Syst. Stab. Control **3**, 827–950 (2017)
7. Kawabe, K., Masuda, M., Nanahara, T.: Excitation control method based on wide-area measurement system for improvement of transient stability in power systems. Electr. Power Syst. Res. **188**, 106568 (2020)
8. Odienat, A., Al Momani, M.M., Alawasa, K., Gharaibeh, S.F.: Low frequency oscillation analysis for dynamic performance of power systems. In: 2021 12th International Renewable Engineering Conference (IREC), pp. 1–6. IEEE (2021)
9. Castillo, O., Amador-Angulo, L.: A generalized type-2 fuzzy logic approach for dynamic parameter adaptation in bee colony optimization applied to fuzzy controller design. Inf. Sci. **460**, 476–496 (2018)
10. Douidi, B., Mokrani, L., Machmoum, M.: A new cascade fuzzy power system stabilizer for multi-machine system stability enhancement. J. Control Autom. Electr. Syst. **30**(5), 765–779 (2019)
11. Iqbal, S., Ayyub, M.: Improved performance of fuzzy logic controller to control dynamical systems: a comparative study. In: 2018 International Conference on Computational and Characterization Techniques in Engineering & Sciences (CCTES), pp. 122–126. IEEE (2018)
12. Ray, P.K., et al.: Firefly algorithm scaled fractional order fuzzy PID based PSS for transient stability improvement. In: 2018 19th International Carpathian Control Conference (ICCC), pp. 428–433. IEEE (2018)
13. Ray, P.K., et al.: A hybrid firefly-swarm optimized fractional order interval type-2 fuzzy PID-PSS for transient stability improvement. IEEE Trans. Ind. Appl. **55**(6), 6486–6498 (2019)
14. Rehman, M., Rahman, J.: Design of real-time fuzzy logic PSS based on PMUs for damping low-frequency oscillations. Master thesis (2016)
15. Verrelli, C.M., Marino, R., Tomei, P., Damm, G.: Nonlinear robust coordinated PSS-AVR control for a synchronous generator connected to an infinite bus. IEEE Trans. Automat. Contr. **67**(3), 1414–1422 (2021)
16. Tzafestas, S.G., et al.: Fuzzy logic applications in engineering science. Microprocess.-Based Intell. Syst. Eng. **29**, 11–30 (2006)
17. Lilly, J.H.: Fuzzy Control and Identification, 1st edn. Wiley, Hoboken (2010)
18. Bakolia, V., Joshi, S.N.: Design and analysis of fuzzy logic based power system stabilizer. Int. J. Eng. Res. Technol. **9**(08), 414–418 (2020)
19. Cherniy, S.P., Susdorf, V.I., Buzikayeva, A.V.: Modeling of an advanced fuzzy logic controller with elementary links in the internal cascade. In: 2020 International Multi-Conference on Industrial Engineering and Modern Technologies (FarEastCon), pp. 1–5. IEEE (2020)
20. Kassie, W.M., Rao, D.G.S.K.: Power system dynamic stability enhancement based on facts device and fuzzy logic controller based stabilizer. Int. Res. J. Eng. Technol. **4**(10), 104–111 (2017)